# Modeling dynamic behavior of nailed soil slope

A. Sengupta
*Indian Institute of Technology Kharagpur, Kharagpur, W.B. 721302, India*

D. Giri
*Parala Maharaja Engineering College, Sitalapalli, Berhampur, Orissa, India*

**Abstract**

Documented performances of soil-nailed system are almost nonexistent in the literature. Most of the literature on nailed soil structures emphasizes on the mechanism of reinforcement and the design of structures under static load only. An analytical method is presented here based on the kinematics theorem of limit analysis to study the stability of reinforced slopes under the seismic loading condition. A circular failure surface, is considered in this study. The proposed method can be viewed as an extension of the method of slices, but it provides a more accurate treatment of forces because they are represented in an integral form. The factor of safety and nail forces obtained by the proposed method have been shown to be in good agreement with the published results for an 8 m high vertical soil nail wall.

## 1 INTRODUCTION

Soil nailing is one of the recent techniques available for stabilizing in-situ soil slopes or cuts. The process of soil nailing includes installation of nails in excavated cuts or in slopes either by driving or grouting in predrilled holes. Stability of the slope face between nails is ensured by providing thin layers of shotcrete reinforced with wire mesh. The nails are generally steel bars, metal tubes or other metal rods that can resist not only tensile force but also shear stress and bending moment. The nailing method has been used in both granular and cohesive soils and in relatively heterogonous deposits.

The general idea among the practicing engineers is that soil-nailed walls perform reasonably well under seismic condition. However documented performances of soil-nailed system are almost nonexistent in the literature. Most of the literature (Gassler 1988, Sakaguchi 1996, Koseki et al. 1998, Matsuo et al. 1998 and, Sivakumar and Singh 2008) on nailed soil structures emphasizes on the mechanism of reinforcement and the design of structures under static load only. The failure mechanisms for slopes under static loading have typically been extended to stability analysis of slopes under seismic loading using pseudo-static approach (Mononobe and Matsuo 1997), but the effect of seismic excitation on the failure pattern of slopes are not addressed. Limited data on the earthquake resistance and corresponding failure mechanisms for steep nailed slopes are available to date. The seismic resistance and the failure mechanism of nailed soil slope during an earthquake event are not clearly understood and need to be investigated properly.

The finite element method is certainly the most comprehensive approach to analyze the performance of soil-structures subjected to seismic loading. However it requires accurate measurement of the properties of the component materials, which are often difficult to achieve. In addition, further difficulties arise from modeling failure in frictional materials. The majority of the existing methods of design and analysis of soil-nailed system are based on the pseudo-static approach, where the effect of earthquake on a potential failure soil mass is represented by horizontal force acting at the centre of gravity. The horizontal force is calculated as the product of a seismic intensity coefficient and the weight of the potential sliding mass. The stability of soil structures under this force is expressed by a factor of safety which is usually defined as the ratio of the resisting force to the destabilizing force. Failure occurs when the safety factor drops below one. However, pseudo-static analysis is generally considered conservative, since even when factor of safety drops below one, the soil structures could experience a finite displacement rather than a complete failure. An alternative analytical method is presented here based on the kinematics theorem of limit analysis to study the stability of reinforced slopes under the seismic loading condition. The kinematic theorem (Juran et al. 1988, 1990) states that slopes will collapse if the rate of work done by external loads and body forces exceed the energy dissipation rate for any assumed kinematically admissible failure mechanism. Soil deformation is assumed to be plastic and failure is associated with the Coulomb's yield condition.

In the present approach, the following assumptions are made:

1. The effect of pore pressure build-up and change of soil strength due to earthquake shaking are ignored. In most cases, weep holes are provided in the walls for safe drainage of water from behind the wall. Also, the backfill soil is usually chosen as cohesionless and free draining material.
2. The slope made of homogeneous cohesionless soil. Strictly speaking, soil is not a homogeneous material. But it is often assumed to be one, only to simplify the calculations in hand.
3. The reinforcement layers are finite in number and have same length. Seldom, nails of different length and dimension are utilized in a wall construction.
4. The resistance to shear, bending and compression is ignored. The nails are typically not designed for bending and compressional loads.
5. The critical failure surface is assumed to pass through the toe of the slopes. The shallow failure surfaces, palling of face wall are ignored as they may not necessarily represent the critical case.
6. The available pullout resistance is assumed to be either the bond strength between soil-reinforcement or the tensile strength of the reinforcement, whichever is smaller. This is a very common assumption in the traditional design of bond length.

Under the above assumptions, the reinforcements provide tensile forces acting in the horizontal direction. The rate of external work is due to soil weight and inertia force induced by the earthquake and the only contribution to energy dissipation is that provided by the reinforcement.

## 2 METHODS OF ANALYSIS

An analytical method based on the kinematics limit equilibrium (Juran et al. 1988, 1990) is presented for the stability analysis of nailed soil slopes. It is assumed in kinematic approach of limit analysis that the soil and the reinforcements are perfectly plastic and their deformation is governed by associated flow rule.

Mathematically, $\dot{\varepsilon}_{ij}^{pl} = \lambda \dfrac{\partial f(\sigma_{ij})}{\partial \sigma_{ij}}$

$$\lambda \geq 0 \quad \text{if} \quad f = 0 \quad \text{and}$$
$$\lambda = 0 \quad \text{if} \quad f < 0 \qquad (1)$$

Where, $\dot{\varepsilon}_{ij}^{pl}$ is the plastic strain rate tensor in a kinematically admissible velocity field, $\sigma_{ij}$ is the stress tensor associated with strain rate tensor, $\lambda$ is a non-negative scalar multiplier and $f(\sigma_{ij}) = 0$ is the yield criteria. Mohr-coulomb failure criteria are assumed and the discontinuity vector (velocity jump) is assumed to be inclined to the rupture surface at the angle of internal friction, $\phi$.

The kinematics theorem of limit analysis (Juran et al. 1988, 1990) states that when the rate of work done by the external forces and the body forces exceeds the rate of internal dissipation energy, the structure will collapse. Micholowski (1998) represented mathematically this theorem as:

$$\int_V D(\dot{\varepsilon}_{IJ})dV \geq \int_S T_i v_i dS + \int_V \gamma_i v_i dV \qquad (2)$$

The left hand side of the equation represents the rate of energy dissipation ($D$) during an incipient failure of a structure and the right hand side includes the rate of work done by all the external forces. In the above equation, $T_i$ is the stress vector on the boundary $S$, $v_i$ is the velocity vector in the kinematically admissible mechanism. $\gamma_i$ is the specific weight and $V$ is the volume of the mechanism. (Refer to Fig. 4). The mathematical form of the theorem states that the rate of energy dissipation is not less than the rate of work done by external forces in any kinematically admissible failure mechanism. The total force on the boundary, $S$, can be calculated only if velocity, $v_i$, on this boundary is constant. If the geometry of the structure is given and all loads and material parameters are known, the safety factor can be calculated. Earthquake effects are considered in terms of seismic coefficient-dependent horizontal forces. Two kinds of failure surfaces are considered in this study, a planar failure surface and a circular failure surface. The proposed method is an extension of the method of slices (Duncan & Wright 2005), but it provides a more accurate treatment of forces because they are represented in an integral form.

### 2.1 Circular Failure Surface

Figure 1 shows a potential circular failure surface AB with centers ($a$, $b$) and radius $r$. Earthquake effect is approximated by a horizontal force equal to $K_h G$ acting through the centre of gravity of the soil wedge.

A number of vertical slices are assumed. The free body diagram of a typical vertical slice *defg* is shown

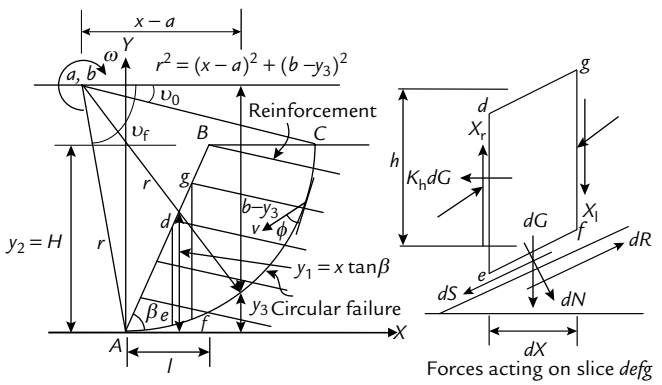


**Figure 1** Circular failure mechanism.

in Figure 1. The self weight of the slice is given by $dG = \gamma h dx$, where $dx$ is the elemental width of slice. The inter-slice forces and acting on *de* and *fg* respectively are equal and opposite and parallel to the base of slice *ef*. $\sum(X_l - X_r)$ is zero for the whole failure mass.

Resolving the forces acting on the base of slice *ef*,

$$dN = \gamma h dx \cos\theta - K_h \gamma h dx \sin\theta \tag{3}$$

$$dS = \gamma h dx \sin\theta + K_h \gamma h dx \cos\theta \tag{4}$$

$$\text{Where } \theta = \sin^{-1}\frac{x-a}{r} \text{ and } r = \sqrt{a^2+b^2} \tag{5}$$

The force $dN$ can produce a maximum shearing resistance $dR$ given by:

$$dR = c dx \sec\theta + \gamma h dx(\cos\theta - K_h \sin\theta)\tan\phi \tag{6}$$

where, $c$ is the cohesion of the soil.

The equation of line, *AB*, in Figure 1, is

$$y_1 = x\tan\beta \tag{7a}$$

The equation of line *BC* is

$$y_2 = H \tag{7b}$$

The equation of the circular failure surface ***AC*** is

$$y_3 = b - \sqrt{r^2-(x-a)^2} \tag{7c}$$

Then the total rate of work done can be equal to the sum of work done by $dS$ and is given by

$$\dot{W} = \gamma v \cos\phi \left[ \sin\theta \left\{ \int_0^l (y_1 - y_3)dx + \int_l^L (H - y_3)dx \right\} + K_h \cos\theta \left\{ \int_0^l (y_1 - y_3)dx + \int_l^L (H - y_3)dx \right\} \right]$$

$$= \gamma v \cos\varphi \, (I_s + K_h I_c) \tag{8}$$

Where,

$$I_s = \int_0^l (y_1 - y_3)\sin\theta dx + \int_l^L (y_2 - y_3)\sin\theta dx$$

$$= \frac{H^2}{2}[(a\cot\beta + b) - \tfrac{H}{3}\operatorname{cosec}^2\beta] \tag{9}$$

$$I_c = \int_0^l (y_1 - y_3)\cos\theta dx + \int_l^L (y_2 - y_3)\cos\theta dx$$

$$= \frac{\tan\beta}{6r}[2r^2 + (l-a)^2]\sqrt{r^2-(l-a)^2} + \frac{b\tan\beta}{r}\left(\frac{a^2}{2} + \frac{b^2}{3}\right) + \frac{r}{2}(a\tan\beta - H)\sin^{-1}\left(\frac{l-a}{r}\right) + \frac{r}{2}(a\tan\beta - b)\sin^{-1}\frac{a}{r} - \frac{r}{2}(b-H)\sin^{-1}\left(\frac{L-a}{r}\right) + \frac{1}{6r}[4r^2 L - ab^2 + (L-a)(H-a)^2] \tag{10}$$

Where, $l = \mathrm{H}\cot\beta$ and

$$L = a + \sqrt{r^2-(b-H)^2} \tag{11}$$

The rate of dissipation of internal energy is due to shear resistance and is given by

$$\dot{D} = \int dR v \cos\phi$$

$$= v\cos\phi \left[ \int_0^L c\sec\theta dx + \int_o^l \gamma(y_1 - y_3)(\cos\theta - K_h \sin\theta)\tan\phi dx + \int_l^L \gamma(y_2 - y_3)(\cos\theta - K_h \sin\theta)\tan\phi dx \right.$$

$$= v\cos\varphi[rc\phi + \gamma\tan\varphi(I_c - K_h I_s)] \tag{12}$$

$$\text{Where, } \phi = \sin^{-1}\frac{L-a}{r} + \sin^{-1}\frac{a}{r} \tag{13}$$

For a given slope angle and internal angle of friction, the toe failure is fully described by two parameters $\vartheta_0$ and $\vartheta_f$ as shown in Figure 1. Rapture of the reinforcement is interpreted as a plastic flow process consistent with the flow rule. The energy dissipation rate in a single reinforcement intersecting a velocity discontinuity can be derived assuming that the discontinuity is of finite-thickness, t, with a high velocity gradient as shown in Figure 2.

The reinforcement contributes to the stability of the structures only through its tensile strength (reinforcement resistance to shear, torsion and bending is neglected). The kinematics requires that the velocity jump vector $[v]$ be inclined to the velocity discontinuity at an angle of internal friction $\phi$. The reinforcement is inclined to the velocity discontinuity at an angle $\xi$ as shown in Figure 2. No reinforcement is assumed to be pulled out and sector *PQ* with length $\frac{t}{\sin\xi}$ (where $t$ being the thickness of rupture layer) is subjected to plastic flow. The rate of energy dissipation in a single reinforcement intersecting a velocity discontinuity per unit horizontal spacing of reinforcement may be calculated as:

$$D = \int_0^{\frac{t}{\sin\xi}} T_i \dot{\varepsilon} dx$$

$$= T_i[v]\cos(\xi - \varphi) \tag{14}$$

Where, $T_i$ is the limit tensile force in the reinforcement per unit horizontal spacing and $\dot{\varepsilon}$ is the strain rate in the direction of reinforcement.

The strain rate in the reinforcement is given by:

$$\dot{\varepsilon} = [v]\frac{\cos(\xi - \varphi)}{t\sin\xi} \tag{15}$$

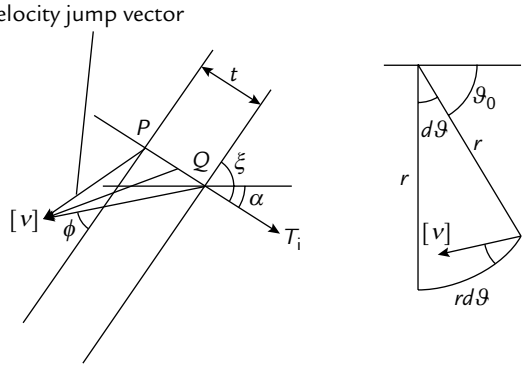


**Figure 2** Velocity jump vector.

The average strength $K_t$ of reinforcement is given by:

$$K_t = nT_i \frac{\cos\alpha}{H} \tag{16}$$

Where, $n$ is the number of reinforcement layers.

The energy dissipation rate per unit area of the discontinuity surface becomes

$$\dot{D} = \int_0^{\frac{t}{\sin\xi}} K_t \sin\xi dx\dot{\varepsilon} \tag{17}$$

$$= K_t[v]\cos(\xi-\varphi)\sin\xi \tag{18}$$

For a circular failure surface, the energy dissipation rate per infinitesimal length ($rd\vartheta$) increment (refer to Figure 2) is given by:

$$d\dot{D} = K_t\dot{\omega}r^2\int\cos(\vartheta+\alpha-\phi)\sin(\vartheta+\alpha)d\vartheta \tag{19}$$

where, $\dot{\omega}$ is the rate of rotation.

Integrating from $\vartheta_0$ to $\vartheta_f$ and assuming $K_t$ to be constant,

$$\dot{D} = K_t\dot{\omega}r^2\int_{\vartheta_0}^{\vartheta_f}\cos(\vartheta+\alpha-\varphi)\sin(\vartheta+\alpha)d\vartheta$$

$$= K_t\dot{\omega}r^2\left[\cos\phi\left\{\frac{\sin^2(\vartheta_0+\alpha)-\sin^2(\vartheta_f+\alpha)}{2}\right\}\right.$$

$$\left.+\sin\phi\left\{\left(\frac{\vartheta_f-\vartheta_0}{2}\right)-\frac{\sin 2(\vartheta_f+\alpha)}{4}+\frac{\sin 2(\vartheta_0+\alpha)}{4}\right\}\right] \tag{20}$$

The total rate of internal energy dissipation is the sum of cohesive and tensile reinforcement forces and is given by

$$\dot{D} = v\cos\phi[rc\varphi+\gamma\tan\phi(I_c-K_hI_s)]$$

$$+K_t\dot{\omega}r^2\left[\cos\phi\left\{\frac{\sin^2(\vartheta_0+\alpha)-\sin^2(\vartheta_f+\alpha)}{2}\right\}\right.$$

$$\left.+\sin\phi\left\{\left(\frac{\vartheta_f-\vartheta_0}{2}\right)-\frac{\sin 2(\vartheta_f+\alpha)}{4}+\frac{\sin 2(\vartheta_0+\alpha)}{4}\right\}\right] \tag{21}$$

The factor of safety, $F_s$, is calculated by taking ratio of equations (21) and (8), and is given by

$$F_s = \frac{rc\varphi+\gamma\tan\phi(I_c-K_hI_s)}{\gamma(I_S+K_hI_c)}$$

$$+K_tr\left[\frac{\left\{\frac{\sin^2(\vartheta_0+\alpha)-\sin^2(\vartheta_f+\alpha)}{2}\right\}}{\gamma(I_s+K_hI_c)}\right.$$

$$\left.+\frac{\tan\phi\left\{\frac{\vartheta_f-\vartheta_0)}{2}-\frac{\sin 2(\vartheta_f+\alpha)}{4}+\frac{\sin 2(\vartheta_0+\alpha)}{4}\right\}}{\gamma(I_S+K_hI_c)}\right] \tag{22}$$

It may be observed from the Equation (22) that the factor of safety for a given slope is a function of parameters like coordinate of failure circle (*a, b*), angle and $\vartheta_0$, and $\vartheta_f$ angle α. Thus minimum value of $F_s$ can be found using the minimization technique.

## 3 VERIFICATION OF THE PROPOSED METHOD

The published results reported by Sivakumar and Singh (2008) for a soil-nailed wall supporting a vertical cut of 8 m high under seismic condition are utilized here to verify the present method of analysis. The geometry of the soil nailed wall supporting the vertical cut is shown in Figure 3. The 8 m high wall was designed in conventional manner by using the allowable stress design procedure. The soil nails were 4.7 m long and placed in 100 mm diameter drill holes. They were grouted in place at 1m apart at an angle of 15° with the horizontal axis. The wall was analyzed numerically by using finite element method. The seismic record from Bhuj (Iyengar and Raghu Kanth 1991) and Uttarkashi (Chandrasekaran and Das 1992) earthquakes was utilized in the reported pseudo-static and dynamic analyses of the wall. The external failure mode of the nailed soil wall in terms of global stability and sliding stability were studied under static, pseudo-static as well as dynamic conditions. In this study, the published pseudo-static results reported in the paper are compared with the results of the present analysis. The horizontal seismic coefficient, $k_h$ for the pseudo-static analysis corresponding to the Bhuj and Uttarkashi earthquake are adopted from the paper and given by 0.106 and 0.241, respectively. All other material parameters adopted from the literature (Sivakumar and Singh 2008) and utilized in the present analysis are given in Table 1.

Since the critical failure surface in the backfill is not given in the referred paper, it is found out by minimization technique and shown in Figure 3.

The factor of safety corresponding to the failure surface is first calculated from Equation 22. The total rate of internal energy dissipated is reduced from the corresponding factor of safety value. From the total energy dissipated value, the rate of internal

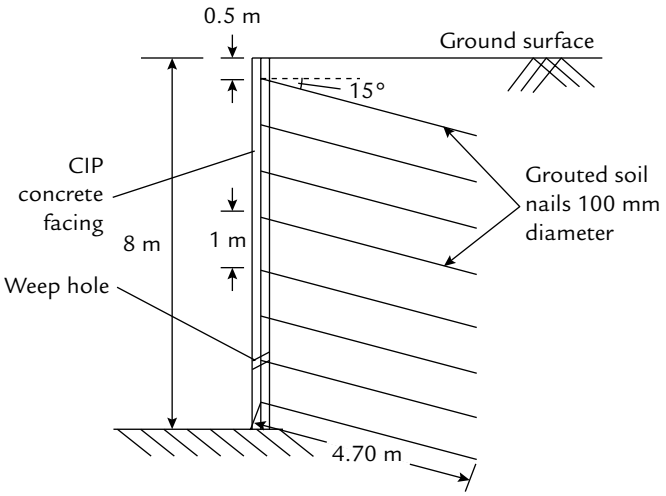


**Figure 3** Geometry of the soil-nailed wall supporting an 8 m vertical cut.

**Table 1** Material parameters for the soil nailed wall

| Parameter | Value |
|---|---|
| Cohesion, $c$(kPa) of the backfill soil | 1.0 |
| Friction angle, $\phi$(degree) of the backfill soil | 30.0 |
| Unit weight, $\gamma$(kN/m$^3$) of the back-fill soil | 16.0 |
| Slope angle, $\beta$(degree) | 0.0 |
| Angle of inclination of nails, $\alpha$ (degrees) | 15.0 |
| Nail length (m) | 4.7 |
| Maxm. axial tensile capacity of nails, $T_i$ (kN) | 83.44 |

**Table 2** Comparison of present method of analysis with published results

| Parameters | Published results from Sivakumar & Singh (2008) | | Results from the present method of analysis | |
|---|---|---|---|---|
| | Bhuj eq. | Uttarkashi eq. | Bhuj eq. | Uttarkashi eq. |
| Maximum axial force in nail, $T_{max}$, (kN) | 34.5 | 40.7 | 32.4 | 37.98 |
| Factor of safety against stability | 0.95 | 0.81 | 0.91 | 0.78 |

energy dissipated due to tensile reinforcement force is obtained. From Equation 16, the tensile force in the reinforcements is calculated. In the above calculations, the velocity jump vector [v] is kept constant, as factor of safety value is independent of velocity jump. Table 2 shows the comparison between the published results and the results from the present theory.

The factor of safety against global stability of the nailed wall for the Bhuj and Uttarkashi earthquakes is found to be 0.91 and 0.78, respectively. These values are comparable with the corresponding published results (0.95 and 0.81). The maximum axial force in the nails as predicted by the present method is found to be 32.4 kN and 37.98 kN, respectively for the Bhuj and Uttarkashi earthquakes. These values are also comparable with the corresponding published results.

## 4 CONCLUSIONS

An analytical method based on kinematic limit approach is developed for stability analysis of soil nailed slopes. Two kinds of failure surfaces, a planar and a circular failure surface, are considered in the formulation. The proposed method can be viewed as an extension of the method of slices, but it provides a more accurate treatment of forces because they are represented in an integral form. The published result of a soil nail wall supporting a vertical cut of 8 m high is utilized to verify the performance of the new methodology. The maximum axial force in the nails and the factor of safety predicted by the proposed method are found to be in good agreement with the corresponding published results for the 8 m high soil nailed vertical cut under seismic conditions.

## REFERENCES

Chandrasekaran, A.R. and Das, J.D. 1992. Analysis of strong ground motion accelerograms of Uttarkashi earthquake of October 20, 1991. *Bull. Indian Soc. Earthquake Tech.* 29(1): 35–55.

Duncan, J.M. and Wright, S.G. 2005. *Soil Strength and Slope Stability*. John Wiley & Sons.

Gassler, G. 1988. Soil nailing- Theoretical basis and practical design. *Proceedings of a conference on Geotechnical. Symposium Theory and Practice of Earth Reinforcement, Japan*. 283–288.

Iyengar, R.N. and Raghu Kanth. S.T.G. 2002. Strong ground motion at Bhuj city during the Kutch earth-quake. *Current Science* 82(11): 1366–1372.

Juran, I., George, B., Khalid, F. and Elias, V. 1988. Kinematical limit analysis approach for the design of nailed soil retaining structures. *Proceedings Geotechnical Symposium on Theory and Practice of Earth Reinforcement, Japan*. 301–306.

Juran, I., George, B., Khalid, F. and Elias, V. 1990. Kinematical limit analysis approach for the design of soil nailed structures. *Journal of Geotechnical Engineering, ASCE* 116(1): 54–71.

Koseki, J., Munaf, Y., Tatsuoka, F., Tateyama, M., Kojima, K. and Sato, T. 1998. Shaking and tilt table tests of geosynthetic reinforced soil and conventional type retaining walls. *Geosynthetic International* 5(1–2): 73–96.

Matsuo, O., Tsutsumi, T., Yokoyama, K. and Saito, Y. 1998. Shaking table tests and analyses of geosynthetic-reinforced soil retaining walls. *Geosynthetic International* 5(1–2): 97–126.

Michalowski, R.L. 1998. Soil Reinforcement for Seismic design of geotechnical structures. *Computers and Geotechnics* 23: 1–17.

Mononobe, N. and Matsuo, H. 1997. On the determination of earth pressure during earthquake. *Proceeding of the World Engineering Conference, Tokyo, Japan*, 176.

Sakaguchi, M. 1996. A study of the seismic behavior of geosynthetic-reinforced walls in Japan. *Geosynthetic International*. 3(1): 13–30.

Sivakumar Babu, G.L. and Singh, V.P. 2008. Numerical Analysis of Performance of Soil Nail Walls in Seismic Condition, *ISET Journal of Earthquake Technology* 45(1–2): 31–40.